Photon echoes of polyatomic molecules in condensed phases

Yi Jing Yan
Department of Chemistry, University of California, San Diego, La Jolla, California 92093-0339
Shaul Mukamel[a)]
Department of Chemistry, University of Rochester, Rochester, New York 14627

(Received 27 July 1990; accepted 26 September 1990)

A theory of optical echo spectroscopies of large polyatomic molecules in condensed phases is developed. Using phase space correlation functions, we examine the interrelationships among the following optical measurements: ordinary photon echo, stimulated photon echo, accumulated photon echo, incoherent accumulated photon echo, and pump–probe absorption. Conditions for the elimination of inhomogeneous broadening in these experiments are specified. A multimode Brownian oscillator model is used to account for high frequency molecular vibrations, as well as solvent modes, and electronic dephasing processes. The effects of quantum beats, spectral diffusion, and homogeneous dephasing on the echo signals are studied and compared in detail with pump–probe and hole burning spectroscopy.

I. INTRODUCTION

Ordinary optical line shapes of molecular systems in condensed phases are usually dominated by electronic inhomogeneous broadening resulting from the variation of local environments of different molecules.[1,2] As a result, the useful structural and dynamical information is hidden underneath a broad inhomogeneous envelope, which makes it impossible to extract this information using linear optical measurements. This state of affairs is typical for spectra in solution, liquids, glasses, polymers, proteins, and molecular crystals. However, nonlinear optical techniques provide the possibility of eliminating inhomogeneous broadening and extracting valuable dynamical information, even when linear optical measurements fail.

The most common spectroscopic techniques used to probe molecular dynamics and optical dephasing processes by selectively eliminating inhomogeneous broadening are fluorescence line narrowing,[3–6] hole burning[7–9] pump–probe absorption,[10–15] and photon echoes [two-pulse photon echo (PE),[16–18] three-pulse stimulated photon echo (SPE),[19–21] and accumulated photon echo (APE)[21–23]]. In fluorescence line narrowing experiments, the molecular dynamics in the excited electronic state are resolved, whereas in pump–probe absorption, the molecular dynamics in the ground electronic state are resolved as well. Photon echoes are the optical analogs of the corresponding magnetic resonance spin echoes.[24,25] In the accumulated photon echo experiment, two trains of laser pulses with equal spacings are successively applied. This technique is usually applied to systems with a long absorption recovery time. The optical echo signal in this case is then accumulated and detected through an interference with the second pulse train (homodyne detection). The accumulated photon echo signal is identical to the stimulated photon echo signal, provided a homodyne detection scheme is used.[21–23] The echo experiments are time resolved, while the fluorescence and pump–probe absorption can be both frequency and time resolved.

The cw hole-burning spectral line shape of solvated chromophores shows Franck–Condon progressions related to the chromophore vibronic structures, broadened by the width $2\pi/T_2$, with T_2 being the homogeneous dephasing time. In this case, only a small fraction of the solute molecules within the broad inhomogeneous distribution are selectively investigated,[1,2] resulting in the elimination of inhomogeneous broadening. The elimination of inhomogeneous broadening in photon echo spectroscopy is of very different origin. In this case the pulsed excitation process is nonselective and the entire inhomogeneous distribution could be excited. However, the signal results from two propagation periods in which inhomogeneous broadening has an opposite effect which exactly cancels. The dephasing in the first period is followed by rephasing in the second.[16,26] The simplest theory for photon echo spectroscopy assumes a line shape with two broadening mechanisms: homogeneous broadening which originates from very fast motions of the surrounding medium and results in a Lorentzian line shape and inhomogeneous broadening. A more general theory is based on the stochastic model, in which the electronic transition frequency of the solvated chromophore is taken to be a Gaussian–Markovian stochastic variable, characterized by two parameters: the modulation strength Δ and the solvent correlation time Λ^{-1}.[2,27] This model accounts properly for the finite time scale of solvent fluctuations and interpolates continuously from the homogeneous limit ($\Lambda/\Delta \gg 1$) to the inhomogeneous limit ($\Lambda/\Delta \ll 1$).[28] However, solvent relaxation processes associated with solvent fluctuations are completely neglected. Therefore, this simple stochastic model does not account for the dynamical Stokes shift,[5,6,28] which results from the solvent reorganization processes occurring *after* the chromophore excitation. Various microscopic solvation theories have been successfully proposed to interpret the spectral diffusion processes in Stokes shift measurements,[5,6,29–33] such as time-dependent hole burning and

[a)] Camille and Henry Dreyfus Teacher/Scholar.

 0021-9606/91/010179-12$03.00

fluorescence spectra. In these theories, however, the solvation dynamics *during* the optical excitation are neglected by assuming an instantaneous optical transition of the chromophore. This approximation should be relaxed in photon echo measurements, in which the solvation dynamics coupled to the optical excitation is monitored directly when the chromophore is in an electronic coherence.

Nanosecond and picosecond echo experiments have been widely used to probe homogeneous line broadening. The development of light sources with impulsively short (femtosecond) time scales has made it possible to probe coherent chromophore motions in real time.[10–15,34–36] The resulting quantum beats are the signatures of the nuclear motions of the chromophore either in the ground electronic state (e.g., impulsive or pulse-shaped stimulated Raman scattering)[10] or in the electronically excited state (e.g., the impulsive fluorescence),[35] or in both states.[11–15] Most recently, femtosecond echo experiments[36] have shown quantum beats which reflect nuclear motions coupled to the electronic coherence between two electronic states.

We have recently developed a Liouville-space theory for molecular nonlinear optical spectroscopy and calculated the pump–probe[37] and stimulated Raman signals[38] of solvated chromophores with arbitrary temporal envelopes of the laser fields. In this paper, we apply this theory to photon echo spectroscopy and incorporate molecular nuclear motions of the chromophore and the solvent. We assume that only two electronic states, $|g\rangle$ and $|e\rangle$, participate in the optical excitation via the dipole interaction. The Hamiltonian is

$$H_T = H - VE(\mathbf{r},t), \tag{1a}$$

$$H = |g\rangle H_g \langle g| + |e\rangle (H_e + \omega_{eg}) \langle e|, \tag{1b}$$

$$V = \mu(|e\rangle\langle g| + |g\rangle\langle e|). \tag{1c}$$

Here, H_g and H_e are the adiabatic Hamiltonians characterizing the nuclear degrees of freedom of the entire molecular system (solute and the solvent) in electronic states $|g\rangle$ and $|e\rangle$, respectively. ω_{eg} is the 0–0 electronic transition frequency, V is the electronic transition dipole operator, and $E(\mathbf{r},t)$ is the classical external electric field consisting of a sequence of the applied laser pulses, which will be further specified for the various echo measurements. The electronic transition dipole matrix element μ in general depends weakly on the solute nuclear coordinates. For simplicity we hereafter neglect that dependence (the Condon approximation) and set $\mu = 1$.

The rest of the paper is organized as follows. In Sec. II, we present a unified theory for various photon echo techniques, which include ordinary, stimulated, accumulated, and incoherent photon echoes. These echo signals can be expressed as a convolution of a same molecular correlation function with the proper sequence of excitation fields. In Sec. III, we consider ideal impulsive echo experiments which use ultrashort pulses, in which the echo signals are directly related to the molecular correlation function. We then in Sec. IV compare the echo signal with the pump–probe absorption, which is its frequency-domain analog. General transform relations among the pump–probe absorption and various echoes are established without alluding to any particular molecular model. The precise conditions for the existence of such transform relationships are specified. The linear and nonlinear molecular correlation functions relevant for calculating the echo signal are evaluated in Sec. V using the second-order cumulant expansion. These correlation functions are then studied for a multimode Brownian oscillator model. The solvent fluctuations and dissipation are accounted for consistently by using the detailed balance condition. Finally our results are summarized in Sec. VI.

II. CORRELATION FUNCTIONS FOR PHOTON ECHO SPECTROSCOPY

A. Two- and three-pulse photon echoes: Dephasing and rephasing processes

Let us consider first the stimulated photon echo measurement in which three short laser pulses with wave vectors $\mathbf{k}_1$,$\mathbf{k}_2$, and $\mathbf{k}_3$ are sequentially applied to the system. The external field in Eq. (1a) for the stimulated photon echo is given by

$$\begin{aligned} E(\mathbf{r},t) = {} & E_1(t+\tau'+\tau)\exp(i\mathbf{k}_1\mathbf{r} - i\Omega_1 t) \\ & + E_2(t+\tau)\exp(i\mathbf{k}_2\mathbf{r} - i\Omega_2 t) \\ & + E_3(t)\exp(i\mathbf{k}_3\mathbf{r} - i\Omega_3 t) + \text{c.c.} \end{aligned} \tag{2}$$

Here, $E_j(t)$ denotes the temporal envelope of the jth incident pulse, while Ω_j denotes its mean frequency. The three incident pulses are delayed by the time intervals τ' and τ. The stimulated echo pulse, which centers around $t = \tau'$ after the third pulse, is then generated in the direction $\mathbf{k}_S = \mathbf{k}_3 + \mathbf{k}_2 - \mathbf{k}_1$ (cf. Fig. 1).[39] The stimulated echo signal S_{SPE} is given by the total generated echo energy, or the integrated area, as a function of the pulse delay times τ' and τ, i.e.,

$$S_{\text{SPE}}(\tau',\tau) = \int_0^\infty dt\, |P^{(3)}_{\text{SPE}}(\mathbf{k}_S,t)|^2. \tag{3}$$

Here $P_{\text{SPE}}(\mathbf{k}_S,t)$ is the macroscopic polarization of the medium with wave vector $\mathbf{k}_S$ induced by the external fields. The

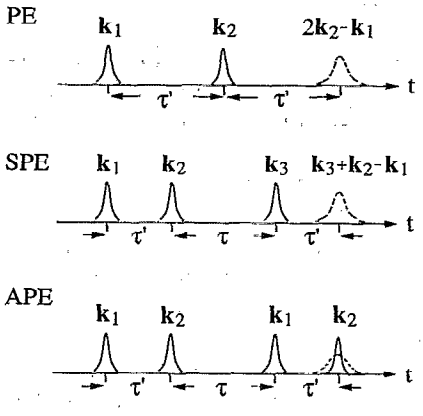

FIG. 1. Pulse sequences for ordinary, stimulated, and accumulated photon echoes, (PE, SPE, and APE, respectively). Shown are the incident pulses (solid curves) and the echo signal (dashed curves). The PE and SPE, signals are detected directly, whereas the APE signal coincides spatially and temporally with the second pulse train with wave vector $\mathbf{k}_2$, and the signal is homodyne detected.

integrand in Eq. (3) represents the temporal profile of the echo signal,[39] which is analyzed in Appendix A. In the weak field limit, we need only consider the polarization to third order in the incident fields. Invoking the rotating wave approximation (RWA) and assuming that the excitation pulses are well separated, we have[40,41]

$$P^{(3)}_{\mathrm{SPE}}(\mathbf{k}_S,t) = i^3\int_0^\infty dt_3\int_0^\infty dt_2\int_0^\infty dt_1\, \mathscr{R}(t_3,t_2,t_1)\chi(t_3-t_1)E_3(t-t_3)E_2(t+\tau-t_3-t_2)E_1^*(t+\tau'+\tau-t_3-t_2-t_1)$$
$$\times\exp[i(\Omega_3+\Omega_2-\Omega_1-\omega_{eg})t_3+i(\Omega_2-\Omega_1)t_2-i(\Omega_1-\omega_{eg})t_1]. \tag{4}$$

Here, we have factorized the total molecular response into two parts, $\mathscr{R}$ and χ, denoting the dynamical contribution and the static (inhomogeneous dephasing) contribution, respectively. In the following we shall show precisely under what conditions the inhomogeneous contribution $\chi(t)$, whose Fourier transform gives the inhomogeneous broadening [cf. Eq. (A4)], is eliminated completely in an echo experiment. The dynamical information is contained in the molecular correlation function

$$\mathscr{R}(t_3,t_2,t_1)\equiv R_2(t_3,t_2,t_1)+R_3(t_3,t_2,t_1) \tag{5a}$$

with

$$R_2(t_3,t_2,t_1)\equiv\mathrm{Tr}[\mathscr{G}_{eg}(t_3)\mathscr{G}_{ee}(t_2)\mathscr{G}_{ge}(t_1)\rho_{gg}], \tag{5b}$$
$$R_3(t_3,t_2,t_1)\equiv\mathrm{Tr}[\mathscr{G}_{eg}(t_3)\mathscr{G}_{gg}(t_2)\mathscr{G}_{ge}(t_1)\rho_{gg}]. \tag{5c}$$

The general nonlinear response function[41] is a sum of four independent molecular correlation functions, $R_\alpha;\alpha=1,...,4$. The echo experiment selects only two of them, R_2 and R_3, which are multiplied by the inhomogeneous dephasing term $\chi(t_3-t_1)$. In the following, we shall show how these two correlation functions account for the rephasing processes which generate the echo. The other two terms, R_1 and R_4, which are multiplied by the inhomogeneous factor $\chi(t_3+t_1)$, exhibit no rephasing processes and do not contribute to the echo. In Eq. (5), we assume that the system is initially in thermal equilibrium in the ground electronic manifold with density matrix ρ_{gg}. Tr denotes a trace over all the nuclear degrees of freedom, which includes both the solvent and the chromophore. The Green function $\mathscr{G}_{mm}(t)$ is defined by its action on an arbitrary operator A:

$$\mathscr{G}_{mn}(t)A\equiv\exp(-iH_mt/\hbar)A\exp(iH_nt/\hbar). \tag{6}$$

The diagonal Green function $\mathscr{G}_{mm}(t_2)$, describes the time evolution of the molecular nuclear degrees of freedom in the electronic state m and has a well-defined classical analog. However, the off-diagonal Green function, $\mathscr{G}_{mn}(t)$ with $m\neq n$, describes the molecular dynamics in an optical coherence (during the t_1 and t_3 periods) which is quantum in nature.[47,49] The diagrammatic representation of stimulated photon echo is given in Fig. 2. The calculation of the correlation functions [Eqs. (5)] for a specific model of nuclear dynamics will be carried out in Sec. V.

The ordinary (two-pulse) photon echo is a special limiting case of the stimulated photon echo in which the third pulse coincides with the second pulse. Its signal, therefore, can be obtained from Eqs. (3) and (4) by simply setting $E_3(t)=E_2(t)$, $\mathbf{k}_3=\mathbf{k}_2$, $\Omega_3=\Omega_2$ and $\tau=0$: (cf. Fig. 1)

$$S_{\mathrm{PE}}(\tau')=S_{\mathrm{SPE}}(\tau',\tau=0). \tag{7}$$

We shall now discuss how the present formalism describes the echo generation by monitoring the rephasing processes of the individual dipoles.[26] This physical picture is simplified if we consider an ideal experiment with infinitely short pulses, $E_j(t)=\delta(t)$. In this case, the echo amplitude [Eq. 4)] is given by $|P_{\mathrm{SPE}}(\mathbf{k}_S,t)|=|\mathscr{R}(t,\tau,\tau')||\chi(t-\tau')|$. The stimulated echo can now be described as follows. At time $t=-(\tau+\tau')$, the initial, ground state, equilibrium density matrix ρ_{gg} is excited by the first impulsive pulse to an optical coherence ρ_{ge}, which then evolves freely as described by the Green function $\mathscr{G}_{ge}(\tau')$. At the time $t=-\tau$ the system interacts with the second impulsive pulse and is transferred to either the electronic ground population ρ_{gg} or excited state population ρ_{ee}. These nonequilibrium population states then evolve freely as described by the Green functions $\mathscr{G}_{gg}(\tau)$ and $\mathscr{G}_{ee}(\tau)$, respectively, until $t=0$ when the system interacts with the third impulsive pulse. The third pulse prepares the system in the optical coherence again and the stimulated echo arises from the free rephasing processes described by the Green function $\mathscr{G}_{eg}(t)$. At $t=\tau'$, the rephasing Green function, $\mathscr{G}_{eg}(\tau')=[\mathscr{G}_{ge}(\tau')]\dagger$, is the Her-

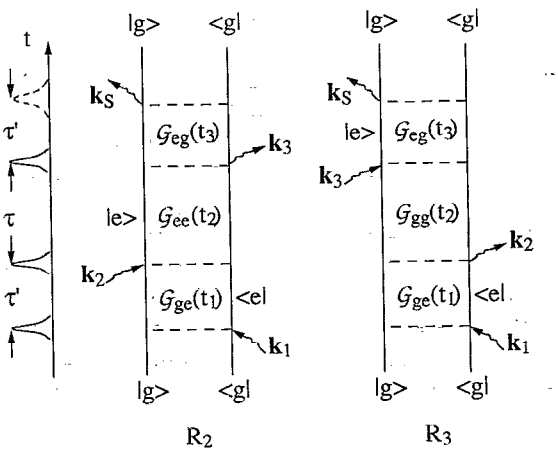

FIG. 2. Feynmann diagrams for stimulated photon echo in the rotating wave approximation. The left (right) diagrams represent the molecular correlation functions $R_2(t_3,t_2,t_1)$ and $R_3(t_3,t_2,t_1)$, respectively [cf. Eqs. (5)]. In a Feynmann diagram (Refs. 39 and 48), the two vertical lines represent the ket and the bra of the density matrix. The wavy arrows denote interactions with the external fields. Time increases from bottom to top. The system is initially at thermal equilibrium in the electronic ground state. At times $t-t_3-t_2-t_1$, $t=t_3-t_2$ and $t-t_3$, the system interacts with the excitation fields with wave vectors $\mathbf{k}_1$, $\mathbf{k}_2$, and $\mathbf{k}_3$, respectively. The echo field with wave vector $\mathbf{k}_S=\mathbf{k}_3+\mathbf{k}_2-\mathbf{k}_1$ is then generated at time t. Between interactions, the system evolves freely as indicated by the Green function [cf. Eq. (6)]. The t_1, t_2, and t_3 time intervals are restricted to $|\tau'\pm\tau_p|$, $|\tau'\pm\tau_p|$, and $|\tau'\pm\tau_p|$, respectively, with τ_p being the time scale of the external pulses.

mitian conjugate of dephasing Green function between the first and the second pulses, and the echo reaches its maximum with $\chi(t-\tau'=0)$ and the effect of the inhomogeneous dephasing is eliminated. For $t>\tau'$, dephasing takes place and the echo decays. The selective elimination of inhomogeneous dephasing by rephasing processes is the key characteristic of echo experiments.[26] As indicated earlier, there are two additional correlation functions, R_1 and R_4 associated with the inhomogeneous dephasing $\chi(t_3+t_1)$, which contribute to a general four-wave-mixing signal (see Appendix B). However, these additional correlation functions do not contribute to the echo signal.

B. Accumulated photon echoes with coherent light sources

We now turn to consider the accumulated photon echo, in which the sample is irradiated with two noncollinear trains of coherent laser pulses. We shall denote the first train as the pump train and the second as the probe train. The latter is delayed with respect to the former by time τ'. The pulse spacing in both trains is $\tau+\tau'$. Each pulse in the pump (probe) train has the wave vector $\mathbf{k}_1$ ($\mathbf{k}_2$), frequency Ω_1 (Ω_2), and a temporal envelope $E_1(t)$ [$E_2(t)$]. The echoes stimulated by the pump train appear at the probe train wave vector $\mathbf{k}_S=\mathbf{k}_1+\mathbf{k}_2-\mathbf{k}_1=\mathbf{k}_2$, are coincident temporally, and oscillate in phase with the probe train. The accumulated echo corresponds therefore to a *homodyne* detection mode whereby the signal is combined with a carrier beam with the same frequency. The multipulse accumulation and the homodyne detection make this technique particularly sensitive and it has been widely used to probe intersystem crossing, vibronic dephasing and relaxation dynamics.[22,23] In this section we shall focus on the accumulated echo measurement of our model system [Eq. (1)] with long excited state lifetime. Consider a complete cycle of four successive pulses; two from the pump train and two from the probe train. The echo field is in this case the same as the stimulated echo generated from the first three (pump–probe–pump) pulses. The relevant polarization is therefore the same as $P^{(3)}_{\rm SPE}(\mathbf{k}_S=\mathbf{k}_1+\mathbf{k}_2-\mathbf{k}_1,t)$ [Eq. (4)] with $E_3=E_1$ and $\Omega_3=\Omega_1$. However, the echo field, in this case, interferes in phase with the fourth (probe) pulse, and the signal is given by[42] (cf. Fig. 1)

$$
\begin{aligned}
S_{\rm APE}(\tau',\tau) &= -2\,{\rm Im}\int_{-\infty}^{\infty} dt\, E_2^*(t-\tau')P^{(3)}_{\rm SPE}(\mathbf{k}_S=\mathbf{k}_1+\mathbf{k}_2-\mathbf{k}_1,t)\\
&= 2\,{\rm Re}\int_{-\infty}^{\infty} dt\int_0^{\infty} dt_3\int_0^{\infty} dt_2\int_0^{\infty} dt_1 \mathscr{R}(t_3,t_2,t_1)\chi(t_3-t_1)\\
&\quad\times E_2^*(t-\tau')E_1(t-t_3)E_2(t+\tau-t_3-t_2)E_1^*(t+\tau+\tau'-t_3-t_2-t_1)\\
&\quad\times\exp[i(\Omega_2-\omega_{eg})t_3+i(\Omega_2-\Omega_1)t_2-i(\Omega_1-\omega_{eg})t_1]. \qquad (8)
\end{aligned}
$$

In most applications of the technique, the train repetition of the four-pulse sequence simply amplifies the echo signal which is given by Eq. (8). Complications may occur when the system is characterized by a broad distribution of relaxation time scales including very long time scales as is the case, e.g., in glasses.[43] In this case slow *spectral diffusion* processes can take place, and their incorporation requires a more elaborate theory which depends on higher order response functions. This extension is beyond the scope of the present article. As a rule, the four-pulse description of the accumulated photon echo is valid provided the time scale τ can be made longer than any other relaxation time scale of the system.

C. Accumulated photon echoes with incoherent light sources

Equation (8) is valid when a mode-locked laser source is used to generate the coherent pump and probe pulse trains. The accumulated photon echo with the same beam configuration can also be performed using incoherent broad band light sources[43–46] to generate the pump with wave vector $\mathbf{k}_1$ and the delayed probe with $\mathbf{k}_2$. The electric field which enters in Eq. (1a), in this case, is given by

$$
\begin{aligned}
E(\mathbf{r},t) &= E(t+\tau')\exp(i\mathbf{k}_1\mathbf{r}-i\Omega t)\\
&\quad + E(t)\exp(i\mathbf{k}_2\mathbf{r}-i\Omega t)+{\rm c.c.} \qquad (9)
\end{aligned}
$$

The temporal envelope of the incoherent light is assumed to be a complex stochastic stationary Gaussian process with

$$\langle E^*(t+\tau)E(t)\rangle=\theta(\tau)=\theta^*(-\tau), \qquad (10a)$$

$$\langle E(t+\tau)E(t)\rangle=\langle E(t)\rangle=\langle E^*(t)\rangle=0. \qquad (10b)$$

Here $\langle\ldots\rangle$ denotes an average over the stochastic fluctuations and $\theta(t)$ denotes the correlation function of the incoherent laser field with typical time scale τ_c. The echo signal is obtained when τ_c is short compared with the dephasing time of the optical medium and the delay time τ' of the probe field with respect to the pump field. We shall be interested in the accumulated echo signal generated along the $\mathbf{k}_2$ direction and detected as a homodyne beat with the probe field. It is given by (cf. Appendix B):

$$
\begin{aligned}
S_{\rm IAPE}(\tau') &= 2\,{\rm Re}\int_0^{\infty} dt_3\int_0^{\infty} dt_2\int_0^{\infty} dt_1\{\exp[i\Omega(t_3-t_1)]\\
&\quad\times[\theta^*(\tau'-t_3)\theta(\tau'-t_1)\\
&\quad+\theta(t_3+t_2-\tau')\theta^*(t_1+t_2-\tau')]\\
&\quad\times\mathscr{R}(t_3,t_2,t_1)\chi(t_3-t_1)\}. \qquad (11)
\end{aligned}
$$

The temporal resolution of this technique is determined by the light correlation time τ_c, rather than by the pulse durations as in a coherent experiment [Eq. (8)].

III. IMPULSIVE PHOTON ECHOES

In the previous section we presented general expressions for photon echo spectroscopy which account for arbitrary molecular dynamical time scales and pulse durations. We shall now consider ideal ultrafast echo experiments for which the calculations are greatly simplified.

In the *impulsive limit*, the laser time scale (the pulse duration for coherent light or the correlation time for incoherent light) is short compared with the molecular vibrational periods and the time scales of homogeneous dephasing and solvent reorganization processes. This is the case for the recent echo experiment performed by Shank and co-workers using 6 fs laser pulses.[36] A second simplifying condition is the *large inhomogeneous broadening limit* whereby the inhomogeneous dephasing time, or the inverse linewidth of inhomogeneous broadening, is short compared to all the dynamical time scales of the system. This is usually the case in condensed phase spectroscopies. Neglecting some trivial prefactors, the echo signals when both limits hold are given by

$$S_{\mathrm{PE}}(\tau') = |\mathscr{R}(\tau',0,\tau')|^2, \tag{12a}$$

$$S_{\mathrm{SPE}}(\tau',\tau) = |\mathscr{R}(\tau',\tau,\tau')|^2. \tag{12b}$$

The homodyne echo techniques require only the first condition (impulsive excitation) and regardless of the magnitude of inhomogeneous broadening yield

$$S_{\mathrm{APE}}(\tau',\tau) = \mathrm{Re}[\mathscr{R}(\tau',\tau,\tau')], \tag{12c}$$

$$S_{\mathrm{IAPE}}(\tau') = \int_0^\infty d\tau\, S_{\mathrm{APE}}(\tau',\tau) + \int_0^{\tau'} d\tau\, S_{\mathrm{APE}}(\tau',\tau'-\tau). \tag{12d}$$

In Eqs. (12), the inhomogeneous dephasing χ is completely eliminated. If we neglect the second term in Eq. (12d) (which results from the overlap of the pump and the probe fields in the incoherent configuration) we recover the result of Bai and Fayer.[46]

It should be noted that Eqs. (12) may also hold when the excitation pulses are short compared with the solvation dynamics but long compared with the chromophore time scales. This is typically the case in picosecond experiments where the chromophore is excited to a particular excited vibronic state and only the solvation dynamics are probed in the real time. In this case, $\mathscr{R}$ contains only the solvent contributions[47] [cf. Eq. (A7)].

IV. THE FREQUENCY DOMAIN ANALOG: PUMP–PROBE SPECTROSCOPY

In the Sec. III, we expressed the various echo signals in terms of same molecular correlation function $\mathscr{R}(t_3,t_2,t_1)$. It should be noted that, in general, there is no direct relationship between the stimulated echo and accumulated echo signals, since the former depends on both the real and imaginary parts of the correlation function whereas the latter depends only on the real part. [cf. Eqs. (12b) and (12c)]. We shall turn now to consider the possibility of a direct Fourier transform relation between the optical echoes and a frequency-domain experiment, i.e., pump–probe absorption. By measuring the total energy loss in the probe field, the pump–probe absorption signal S_{PP} is obtained as a function of τ, the delay time of the probe with respect to the pump, Ω_1, the pump frequency, and Ω_2, the probe frequency. The formal expression for S_{PP} is similar to the first equality in Eq. (8), the accumulated photon echo signal. However, the configuration of the excitation fields in pump–probe experiment is different from that in accumulated echo.

In general, the polarization relevant for pump–probe spectroscopy contains both the terms $\mathscr{R}(t_3,t_2,t_1)\chi(t_3-t_1)$ and $\bar{\mathscr{R}}(t_3,t_2,t_1)\chi(t_3+t_1)$ [cf. Eq. (B1)]. This constitutes the doorway/window picture for transient absorption.[37,48] Therefore, there is no general transform relationship between echo signal and probe absorption measurement. However, in a medium with large inhomogeneous broadening, we may approximate the inhomogeneous dephasing function $\chi(t)$ by a delta function. In this case the $\bar{\mathscr{R}}$ term in the Condon approximation becomes independent of t_2 and does not contribute to the transient absorption (it simply provides a dc background). If we further assume that both pump and probe pulses are long compared to the electronic dephasing time but short compared to the molecular nuclear dynamics, the probe absorption signal is insensitive to the temporal characteristics of the incoming fields.[37,48] In this case, the pump–probe signal, up to a trivial prefactor, is given by

$$S_{\mathrm{PP}}(\tau;\Omega_2-\Omega_1) = \mathrm{Re}\int_0^\infty dt \times \exp[i(\Omega_2-\Omega_1)t]\,\mathscr{R}(t,\tau,t). \tag{13}$$

In this case the inhomogeneous contribution is completely eliminated. Equation (13) is also valid when the excitation pulses are short compared to the solvation dynamics but long compared to the chromophore time scales. In this case, $\mathscr{R}$ in Eq. (13) contains only the solvent dynamics and the pump–probe absorption is then referred to as hole burning.[37,47]

Equations (12b), (12c), and (13) constitute our theoretical basis for analyzing the intrinsic relations among the stimulated photon echo S_{SPE}, the accumulated photon echo S_{APE} and the pump–probe absorption S_{PP} of a system with large inhomogeneous broadening. All three optical signals depend on the same molecular correlation function $\mathscr{R}$. In general, this correlation function is complex and has two independent (real and imaginary) components. Equations (12b), (12c) and (13) can, therefore, be used to obtain a general transform relation among the three optical signals, S_{SPE}, S_{APE}, and S_{PP}, which is not restricted to any specific molecular model. Especially, when the delay time is long compared with the time scales of the molecular nuclear relaxation processes, i.e., $\tau > \tau_R$, we can factorize R_2 and R_3 as[49]

$$R_2(t,\tau>\tau_R,t) = J_e(t)\exp(-\gamma\tau)J_g^*(t), \tag{14a}$$

$$R_3(t,\tau>\tau_R,t) = J_g(t)\exp(-\gamma'\tau)J_g^*(t) \approx J_g(t)J_g^*(t) \tag{14b}$$

with

$$J_u(t) = \mathrm{Tr}[\mathscr{G}_{eg}(t)\rho_u]; \quad u = e \text{ or } g. \tag{14c}$$

Here, γ and $\gamma'(\simeq 0)$ represent the inverse lifetimes of the electronic excited and ground states, respectively. $J_u(t)$ is the molecular linear response function with respect to the thermal equilibrium distribution in the $|u\rangle$ electronic states. The Fourier transforms of $J_g(t)$ and $J_e(t)$ give, respectively, the stationary absorption and fluorescence line shapes.[49] These functions satisfy the symmetry relations: $J_u(-t) = J_u^*(t)$ and $R_\alpha(-t,\tau>\tau_R,-t) = R_\alpha^*(t,\tau\gtrsim\tau_R,t)$. In this case, Eq. (13) can be expressed as a Fourier transform, resulting in

$$\mathscr{R}(t,\tau>\tau_R,t) = \frac{1}{\pi}\int_{-\infty}^{\infty} d(\Omega_2-\Omega_1)\times\exp[-i(\Omega_2-\Omega_1)t]S_{\rm PP}(\tau>\tau_R;\Omega_2-\Omega_1). \quad (15)$$

Here, τ_R represents the molecular nuclear relaxation time. The stimulated photon echo signal [Eq. (12b)] is therefore related to the amplitude square of the Fourier transform of the pump–probe absorption line shape; whereas, the accumulated photon echo [Eq. (12c)] is related to its cosine transform. We have

$$S_{\rm SPE}(\tau',\tau>\tau_R) = \left|\frac{1}{\pi}\int_{-\infty}^{\infty} d(\Omega_2-\Omega_1)\times\exp[-i(\Omega_2-\Omega_1)\tau']\times S_{\rm PP}(\tau>\tau_R;\Omega_2-\Omega_1)\right|^2, \quad (16a)$$

$$S_{\rm APE}(\tau',\tau>\tau_R) = \frac{1}{\pi}\int_{-\infty}^{\infty} d(\Omega_2-\Omega_1)\times\cos[(\Omega_2-\Omega_1)\tau']\times S_{\rm PP}(\tau>\tau_R;\Omega_2-\Omega_1). \quad (16b)$$

The inverse transform does not exist since $S_{\rm PP}$ depends on the two-sided Fourier transform of the correlation function $\mathscr{R}$. However, if the delay time is longer than the electronic excited lifetime, i.e., $\tau>\gamma^{-1}$, Eq. (14a) reduces to $R_2(t',\tau\to\infty,t') = 0$. This is the case in persistent hole burning experiments.[9] In this case, we have [cf. Eqs. (12c), (12b), and (13)]

$$S_{\rm APE}(\tau',\tau\to\infty) = |J_g(\tau')|^2, \quad (17a)$$

$$S_{\rm SPE}(\tau',\tau\to\infty) = [S_{\rm APE}(\tau',\tau\to\infty)]^2, \quad (17b)$$

$$S_{\rm PP}(\tau\to\infty;\Omega_2-\Omega_1) = \int_0^{\infty} d\tau'\cos[(\Omega_2-\Omega_1)\tau']\times S_{\rm APE}(\tau',\tau\to\infty). \quad (17c)$$

Equation (17c) is consistent with the previous result of Saikan *et al.*[50]

V. APPLICATION TO THE MULTIMODE BROWNIAN OSCILLATOR MODEL

In the previous sections we formulated the various optical echo signals in terms of the molecular four-time correlation functions, R_2 and R_3 [Eqs. (5)]. These functions carry not only the dynamical information when the chromophore is in the excited ($\mathscr{G}_{ee}$) or in the ground ($\mathscr{G}_{gg}$) electronic population state, but also the dynamics when it is in an electronic coherence ($\mathscr{G}_{eg}$ and $\mathscr{G}_{ge}$). We have recently developed a generalized Langevin equation which allows to propagate explicitly these Green functions, $\mathscr{G}_{mn}$ with $m,n = e$ or g, for harmonic and anharmonic chromophores in solution.[41] The correlation function R_α is then obtained by tracing over all the final states (or phase space points) and averaging over the initial distribution.

We shall now present an alternative approach for calculating these correlation functions. This approach is based on a cumulant expansion used to express these four-time correlation functions in terms of a single two-time correlation function. We then evaluate the two-time correlation function using a Brownian oscillator model.

A. The second-order cumulant expansion

The optical response of the system depends directly on the difference of the excited state and the ground state Hamiltonian

$$U \equiv H_e - H_g. \quad (18)$$

It is clear that if $U=0$ the nuclear degrees of freedom do not couple to the optical transition. Performing the cumulant expansion of Eqs. (5) and (14c) around the molecular ground state Hamiltonian H_g, to second order in U, we obtain[2]

$$J_g(t) = \exp[-g(t)], \quad (19a)$$

$$J_e(t) = \exp[-g^*(t)], \quad (19b)$$

$$R_2(t_3,t_2,t_1) = \exp[-g^*(t_3)-g^*(t_1)+g(t_2)-g(t_2+t_3)-g^*(t_1+t_2)+g^*(t_1+t_2+t_3)], \quad (19c)$$

$$R_3(t_3,t_2,t_1) = \exp[-g(t_3)-g^*(t_1)+g^*(t_2)-g^*(t_2+t_3)-g^*(t_1+t_2)+g^*(t_1+t_2+t_3)], \quad (19d)$$

where

$$g(t) = i\lambda t + \int_0^t d\tau_1\int_0^{\tau_1} d\tau_2\,\ddot{g}(\tau_2), \quad (20)$$

and

$$\lambda = \langle U\rangle, \quad (21a)$$

$$\ddot{g}(t) = \langle U(t)U\rangle - \langle U\rangle^2. \quad (21b)$$

In Eqs. (19), we include also the molecular linear correlation functions $J_u(t)$ [Eq. (14c)]. In Eqs. (21), $\langle\ldots\rangle$ denotes an average over the initial equilibrium distribution within the ground electronic state manifolds. $U(t)$ is the operator [Eq. (18)] in the Heisenberg picture with respect to the ground state dynamics:

$$U(t) \equiv \exp(iH_g t)\,U\exp(-iH_g t). \quad (22)$$

Equations (19) are exact for a linearly displaced harmonic oscillation system.[2,41] The key quantity here is $\ddot{g}(t)$ [Eq. (21b)], the two-time correlation function of the operator U. In general, $\ddot{g}(t)$ is a complex function of time. We shall now separate it into its real and imaginary parts:

$$\ddot{g}(t) \equiv \ddot{g}^{(1)}(t) - i\ddot{g}^{(2)}(t), \quad (23)$$

with

$$\ddot{g}^{(1)}(t) = \tfrac{1}{2}[\langle U(t)U\rangle + \langle UU(t)\rangle] - \langle U\rangle^2, \quad (24a)$$

$$\ddot{g}^{(2)}(t) \equiv \frac{i}{2}[\langle U(t)U\rangle - \langle UU(t)\rangle]. \quad (24b)$$

Both $\ddot{g}^{(1)}(t)$ and $\ddot{g}^{(2)}(t)$ are real, since they represent the expectation values of Hermitian operators. Also $\ddot{g}^{(1)}(t) = \ddot{g}^{(1)}(-t)$ is symmetric whereas $\ddot{g}^{(2)}(t) = \ddot{g}^{(2)}(-t)$ is antisymmetric. The fluctuation–dissipation theorem provides a general connection between $\ddot{g}^{(1)}$ and $\ddot{g}_{(2)}$ so that they are not independent. To show that, we introduce the spectral density functions:

$$C(\omega) \equiv \frac{1}{2\pi}\int_{-\infty}^{\infty} dt \exp(i\omega t)\ddot{g}(t)$$

$$= \frac{1}{\pi}\mathrm{Re}\int_0^{\infty} dt \exp(i\omega t)\ddot{g}(t), \tag{25a}$$

$$C^{(+)}(\omega) \equiv \frac{1}{2\pi}\int_{-\infty}^{\infty} dt \exp(i\omega t)\ddot{g}^{(1)}(t)$$

$$= \frac{1}{\pi}\int_0^{\infty} dt \cos\omega t\, \ddot{g}^{(1)}(t), \tag{25b}$$

$$C^{(-)}(\omega) \equiv \frac{1}{2\pi i}\int_{-\infty}^{\infty} dt \exp(i\omega t)\ddot{g}^{(2)}(t)$$

$$= \frac{1}{\pi}\int_0^{\infty} dt \sin\omega t\, \ddot{g}^{(2)}(t). \tag{25c}$$

Here, the second identities are obtained using the symmetry properties. $C^{(+)}(\omega) = C^{(+)}(-\omega)$ is symmetric and $C^{(-)}(\omega) = -C^{(-)}(-\omega)$ is antisymmetric. $C(\omega) = C^{(+)}(\omega) + C^{(-)}(\omega)$ satisfies the detailed balance relation: $C(\omega) = \exp(\hbar\omega/k_BT)C(-\omega)$, which can be directly proven from Eqs. (21b) and (25a) by expressing $\ddot{g}(t)$ in terms of the eigenstates of H_g. These properties result in

$$C(\omega) = \left[1 + \tanh\left(\frac{\hbar\omega}{2k_BT}\right)\right]C^{(+)}(\omega)$$

$$= \left[1 + \coth\left(\frac{\hbar\omega}{2k_BT}\right)\right]C^{(-)}(\omega). \tag{26}$$

Equation (26) is the fluctuation–dissipation theorem which connects the response function with the correlation function.[51] It can be shown that $C(\omega)$,$C^{(+)}(\omega)$, and $\omega C^{(-)}(\omega)$ are non-negative. Performing a Fourier transform on Eqs. (26) followed by a double temporal integration, we obtain

$$g(t) = i\lambda t + \int_{-\infty}^{\infty} d\omega\, \omega^{-2}[1 - i\omega t - \exp(-i\omega t)]$$

$$\times\left[1 + \tanh\left(\frac{\hbar\omega}{2k_BT}\right)\right]C^{(+)}(\omega) \tag{27a}$$

or

$$g(t) = i\lambda t + \int_{-\infty}^{\infty} d\omega\, \omega^{-2}[1 - i\omega t - \exp(-i\omega t)]$$

$$\times\left[1 + \coth\left(\frac{\hbar\omega}{2k_BT}\right)\right]C^{(-)}(\omega). \tag{27b}$$

Here, k_B is the Boltzmann constant and T is the temperature. Equations (27a) and (27b) are useful in the calculation of molecular line shapes in condensed phases, since $C^{(+)}(\omega)$ and $C^{(-)}(\omega)$ have simple classical analogs. This will be used in the next subsection.

B. The Brownian oscillator model

The linearly displaced Brownian harmonic oscillator model[41,52] provided a general and very convenient way for incorporating the coupling of nuclear motions (whether intramolecular or solvent) to the optical transition. In this model, the molecular and solvent nuclear motions are represented by N modes with $U \equiv H_e - H_g = \Sigma_j \omega_j D_j (q_j + D_j/2)$. q_j denotes the dimensionless coordinate and ω_j is its harmonic frequency, while D_j is its dimensionless displacement between the potential surfaces of electronic excited and ground states. In addition we assume that each vibration undergoes a Brownian motion satisfying the generalized Langevin equation:

$$\ddot{q}_j(t) = -\omega_j^2 q_j(t) - \int_0^t d\tau\, \hat{\gamma}_j(t-\tau)\dot{q}_j(\tau) + \omega_j f_j(t). \tag{28}$$

Here, $\hat{\gamma}_j(t)$ is a non-Markovian friction kernel and $f_j(t)$ is a Gaussian stochastic random force due to the effect of solvent environment on the jth mode. The friction and the random force satisfy the fluctuation–dissipation relation $\langle f_j(t) f_k(\tau)\rangle = \delta_{jk}(\bar{n}_j + \frac{1}{2})\hat{\gamma}_j(t-\tau)$. Here $\langle\ldots\rangle$ denotes an average over the stochastic variables. δ_{jk} is the Kronecker delta, and

$$\bar{n}_j = [\exp(\hbar\omega_j/k_BT) - 1]^{-1} \tag{29}$$

is the thermally averaged occupation number of the jth mode. For this model we have

$$g(t) = \sum_j g_j(t). \tag{30}$$

The expression for $g_j(t)$ is similar to Eqs. (27a) or (27b) with replacing λ, $C^{(+)}$, and $C^{(-)}$ by λ_j,$C_j^{(+)}$ and $C_j^{(-)}$, respectively and where

$$C_j^{(+)}(\omega) = (\Delta_j^2/\pi)\int_0^{\infty} dt \cos\omega t\, M_j(t), \tag{31a}$$

$$C_j^{(-)}(\omega) = (\lambda_j/\pi)\int_0^{\infty} dt \sin\omega t\, Z_j(t) \tag{31b}$$

with

$$\Delta_j^2 \equiv \omega_j^2 D_j^2(\bar{n}_j + \tfrac{1}{2}), \tag{32a}$$

$$\lambda_j \equiv \omega_j D_j^2/2, \tag{32b}$$

and

$$M_j(t) \equiv \frac{\frac{1}{2}[\langle q_j(t)q_j\rangle + \langle q_j q_j(t)\rangle] - \langle q_j\rangle^2}{\langle q_j^2\rangle - \langle q_j\rangle^2}, \tag{32c}$$

$$Z_j(t) \equiv i\omega_j[\langle q_j(t)q_j\rangle - \langle q_j q_j(t)\rangle] = -\dot{M}_j(t). \tag{32d}$$

By definition, both $M_j(t)$ and $Z_j(t)$ are real with $M_j(0) = 1$ and $Z_j(0) = 0$. Furthermore, $M_j(\infty) = Z_j(\infty) = 0$ for a dissipative medium. Solving for $M_j(t)$ or $Z_j(t)$ from the Langevin equation [Eq. (28)] and then substituting for Eq. (31), we obtain

$$C_j^{(+)}(\omega) = (\Delta_j^2/\pi)\mathrm{Re}\left[\frac{-i\omega + \gamma_j(\omega)}{-\omega^2 - i\omega\gamma_j(\omega) + \omega_j^2}\right] \tag{33a}$$

or

$$C_j^{(-)}(\omega) = (\lambda_j/\pi)\mathrm{Im}\left[\frac{\omega_j^2}{-\omega^2 - i\omega\gamma_j(\omega) + \omega_j^2}\right], \tag{33b}$$

with

$$\gamma_j(\omega) \equiv \int_0^\infty dt \exp(i\omega t)\dot{\gamma}_j(t). \tag{33c}$$

It can be shown that $g_j(t)$ obtained via Eqs. (27a) and (33a) is not identical to that obtained using Eqs. (27b) and (33b). This arises since the Langevin equation with a classical random force does not satisfy the detailed balance condition.[53] Equations (27) and (33) constitute the main results of this section. Using these results, we may perform the model calculations for the pump–probe signal [Eq. (13)] as well as the various impulsive echo experiments [Eqs. (12)] or for the more general echo measurements (cf. Sec. II).

We shall now calculate the impulsive ordinary photon echo signal [Eq. (12a)] using the present Brownian oscillator model. Making use of Eqs. (28) and (19), we may rewrite Eq. (12a) as

$$S_{\mathrm{PE}}(\tau') = \prod_j S_{\mathrm{PE}}^{(j)}(\tau'), \tag{34a}$$

with

$$S_{\mathrm{PE}}^{(j)}(\tau') = \exp\{-2\mathrm{Re}[g_j(\tau') + 3g_j(\tau') - g_j(2\tau')]\}. \tag{34b}$$

This signal depends only on the real part of g_j.

In Eqs. (34), the product runs over all the system modes which are considered explicitly in the Langevin equation [cf. (Eq. (28)]. In the calculation of molecular optical line shapes in condensed phases, the system modes can be divided into two groups. The first group consists of all the optically active modes of the chromophore or some particular microscopic solvent modes which are strongly coupled to the electronic transition. These modes contribute to the quantum beats in the time domain and to the Franck–Condon progressions in the frequency domain. The second group consists of the macroscopic solvent coordinates representing the intra- or intermolecular solvation shells, such as the electronic solvation coordinate[31] and the intramolecular bath. These motions describe dephasing and spectral diffusion processes, and therefore contribute to the echo decay and the spectral line broadening in the frequency domain.

The optically active modes usually have high vibrational frequencies compared with the solvent friction. Their motions are characterized by the parameters D_j, frequency ω_j and friction γ_j. In the extreme case where the relevant friction is much smaller than the vibrational frequency, $\gamma_j(\omega_j) \ll \omega_j$, we have the exact solutions $M_j(t) = \cos\omega_j(t)$ and $Z_j(t) = \sin\omega_j t$, yielding $C_j^{(+)}(\omega) = \frac{1}{2}\omega^2 D_j^2(\bar{n}_j + \frac{1}{2}) \times [\delta(\omega - \omega_j) + \delta(\omega + \omega_j)]$ and $C_j^{(-)}(\omega) = \frac{1}{4}\omega^2 D_j^2 \times [\delta(\omega - \omega_j) - \delta(\omega + \omega_j)]$. In this case, Eqs. (27a) and (27b) are equivalent, resulting in the well-known expression:[49,54]

$$g_j(t) = -(D_j^2/2)\{(\bar{n}_j + 1)[\exp(-i\omega_j t) - 1] + \bar{n}_j[\exp(i\omega_j t) - 1]\}. \tag{35a}$$

[Once the friction is included and M_j and Z_j are evaluated approximately, Eqs. (27a) and (27b) are no longer the same.] The contribution from the coherent motion with $\gamma_j = 0$ can now be obtained by substituting Eq. (33) for (32b). We obtain

$$S_{\mathrm{PE}}^{(j)}(\tau') = \exp[-4(\bar{n}_j + \tfrac{1}{2})D_j^2(1 - \cos\omega_j\tau')^2]. \tag{35b}$$

Equation (35b) shows that in the impulsive limit the ordinary echo signal results in quantum beats for the coherent motions of the underdamped chromophore modes. This is the case in the recent experiment of Shank and coworkers.[8] It should be emphasized that the coherent motion in an echo experiment is coupled to the electronic transition, and the vibrational frequency of mode j in the electronically excited state may be very different from that in the ground electronic state. The echo beats contain therefore all the possible combinations of these two different frequencies and are modulated by the fast electronic dephasing processes.[36] This is in contrast with the impulsive absorption and stimulated Raman signals where the beats, which reflect the coherent motion in either the excited electronic state or in the ground electronic state, are modulated by the much slower vibrational dephasing processes.[10–15,37,38]

Let us turn now to the second group or the macroscopic solvation coordinates which have usually very low characteristic frequencies compared with the friction, and are overdamped. Their dynamics can then be described using Eq. (26) with $\ddot{q}_j(t) = 0$.[41,52] We shall further invoke the Markovian approximation and set $\gamma(\omega) = \gamma$. We then have $M_j(t) = \exp(-\Lambda_j t)$ and $C_j^{(+)}(\omega) = (\Delta_j^2\Lambda_j/\pi)/(\omega^2 + \Lambda_j^2)$. Using contour integration,[55] Eq. (27a) then results in

$$g_j(t) = (\Delta_j/\Lambda_j)^2[\exp(-\Lambda_j t) + \Lambda_j t - 1][1 - i\tan(\hbar\Lambda_j/2k_BT)] + i\lambda_j t + i(\hbar\Delta_j/\pi k_BT)^2 \sum_{n=0}^{\infty} \frac{4\hbar\Lambda_j/k_BT}{(2n+1)^2[(2n+1)^2\pi^2 - (\hbar\Lambda_j/k_BT)^2]} \times\{\exp[-\pi(2n+1)(k_BT/\hbar)t] + \pi(2n+1)(k_BT/\hbar)t - 1\}. \tag{36a}$$

Alternatively, we can calculate $g_j(t)$ using Eq. (27b). In this case we have $Z_j(t) = \Lambda_j\exp(-\Lambda_j t)$ and $C_j^{(-)}(\omega) = (\omega\lambda_j\Lambda_j/\pi)/(\omega^2 + \Lambda_j^2)$ and therefore

$$g_j(t) = i(\lambda_j/\Lambda_j)[1 - \exp(-\Lambda_j t)] + (\lambda_j/\Lambda_j)\cot(\hbar\Lambda_j/2k_BT)[\exp(-\Lambda_j t) + \Lambda_j t - 1] + \frac{4\hbar^2\lambda_j\Lambda_j}{\pi(k_BT)^2}\sum_{n=1}^{\infty}\frac{\exp[-(2\pi nk_BT/\hbar)t] + (2\pi nk_BT/\hbar)t - 1}{2n[4n^2\pi^2 - (\hbar\Lambda_j/k_BT)^2]}. \tag{36b}$$

Here, we characterize the solvation mode by the parameters λ_j, Δ_j, and Λ_j, representing, respectively, the solvent reorganization frequency, solvent fluctuation amplitude, and the inverse time scale of solvent relaxation. In the high temperature limit $k_B T \gg \hbar\omega$,[41] we have $\hbar\Delta_j^2 = 2k_B T\lambda_j$, and both of Eq. (36a) and (36b) reduce to

$$g_j(t) = (\Delta_j/\Lambda_j)^2[\exp(-\Lambda_j t) + \Lambda_j t - 1] + i(\lambda_j/\Lambda_j)[1 - \exp(-\Lambda_j t)]. \quad (37)$$

This is consistent with the result obtained directly from the generalized Langevin equation for the off-diagonal Green function $\mathscr{G}_{eg}(t)$.[41] If we further neglect the solvent relaxation processes associated with the fluctuation by setting the reorganization parameter $\lambda_j = 0$, we recover the celebrated stochastic model of line broadening.[27]

The solvation dynamics probed by the echo measurement can now be obtained by substituting Eq. (36a) or (36b) in (34b). In the high temperature limit ($k_B T \gg \hbar\omega_j$) we get

$$S_{\mathrm{PE}}^{(J)}(\tau') = \exp\left\{-(4\Delta_j^2/\Lambda_j)\int_0^{\tau'} dt\,[1 - \exp(-\Lambda_j t)]^2\right\}. \quad (38)$$

In the fast modulation (homogeneous) limit where the solvent correlation time $\Lambda_j^{-1} \ll \tau'$ is negligibly small, Eq. (38) reduces to

$$S_{\mathrm{PE}}^{(J)}(\tau') = \exp(-4\tau'/T_2). \quad (39)$$

This is the well-known relation between the echo signal and the homogeneous dephasing time $T_2 \equiv \Lambda_j/\Delta_j^2$. In this limit, the FWHM of the hole-burning spectrum [Eq. (13)] is equal to $4/T_2$. In the slow modulation limit where $\Lambda_j^{-1} \gg \tau'$, Eq. (38) reduces to

$$S_{\mathrm{PE}}^{(J)}(\tau') = \exp[-(\tau'/\tau_0)^3], \quad (40)$$

where $\tau_0 \equiv (\frac{4}{3}\Delta_j^2\Lambda_j)^{-1/3}$. A detailed analysis of the echo decay time and the hole-burning spectral width in the presence of the spectral diffusion was given elsewhere.[46,55]

VI. SUMMARY

In this paper we presented general expressions for the stimulated echo [Eq. (3) with (4)], the ordinary echo [Eq. (7)], the coherent accumulated echo [Eq. (8)], and the incoherent accumulated echo [Eq. (11)] of solvated chromophore molecules, generated using weak laser fields. We considered also the temporal behavior of the echo profile [Eq. (A6)], and expressed it in terms of the excitation fields and the medium inhomogeneity [Eq. (A3)]. We then considered the impulsive limit where the excitation field is short compared with the molecular dynamical time scales (excluding inhomogeneous dephasing). The relevant time scale of the incoherent laser field is the field correlation time, rather than the pulse duration. In the impulsive limit, all the echo signals [Eqs. (12)] are directly related to the molecular correlation function $\mathscr{R}$. We may refer to Eqs. (12) as the bare echo signals.[48] Inhomogeneous broadening is eliminated by the rephasing processes which completely reverse the inhomogeneous dephasing. The bare echo signals are closely related to the bare pump–probe absorption [Eq. (13)], which is obtained when the excitation fields are short compared with the nuclear dynamics but long compared with electronic dephasing.[37,48] Equations (12) and (13) also hold when the field time scale is long compared with the nuclear dynamics of the optically active chromophore motions, but short compared with the solvent relaxation and homogeneous dephasing processes. In this case, only the solvation dynamics are probed; i.e., the molecular correlation functions contain only the solvent contributions [cf. Eq. (A7)].

The pump–probe absorption is the frequency-domain analog of the photon echo, since it is the one-sided-Fourier transform of the echo correlation function [Eq. (13)]. This correlation function is complex, in general. Therefore, there is no completely general relationship between the pump–probe absorption signal to any single echo measurement. However, such transform relations do exist for long delay times [Eqs. (16) and (17)].

We further developed a Brownian oscillator model, which accounts for quantum beats as well as homogeneous dephasing, inhomogeneous dephasing and the spectral diffusion in a unified fashion (Sec. V). The echo beats result from the underdamped Brownian oscillation coupled to the optical coherence [cf. Eq. (34)]. As a result, the echo signal may resolve only the quantum beats of high frequency vibrations,[10] since it is modulated by the fast electronic dephasing processes in condensed phases. Detailed balance is built in through Eq. (27a) or (27b). Therefore, the relationship between the solvent reorganization and fluctuation was established and is consistent with the fluctuation–dissipation theorem. The resulting stationary absorption and emission profiles [the Fourier transform of Eq. (19a) and (19b), respectively] vary continuously from a Lorentzian to a Gaussian form. We presented also the echo decay profile which is exponential $\exp(-a\tau')$ in the fast modulation limit [Eq. (39)] and $\exp(-c\tau'^3)$ in the slow modulation limit [Eq. (40)]. In a real solvent, there is a multitude of solvent time scales which represent the contributions from different solvation shells. These are easily incorporated using the present theory.

It should also be noted that the stationary absorption and emission profiles obtained from the Fourier transform of Eqs. (19a) and (19b) have a mirror symmetry. This is the result of the second-order cumulant expansion in which we expand all the Green functions, $\mathscr{G}_{eg}(t_3), \mathscr{G}_{uu}(t_2)$ with $u = e$ or g, and $\mathscr{G}_{ge}(t_1)$, in Eqs. (5) around the molecular ground state Hamiltonian H_g. An improved cumulant expansion may be obtained by expanding $\mathscr{G}_{eg}(t_3)\mathscr{G}_{uu}(t_2)$ around H_u, while expanding $\mathscr{G}_{ge}(t_1)$ around H_g. Another simple approach is to expand the optically active modes of the chromophore in terms of their vibronic eigenstates,[37] while keeping the cumulant expansion for the overdamped solvent coordinates.

ACKNOWLEDGMENTS

We wish to thank Wayne B. Bosma for useful discussions. The support of the National Science Foundation, the Air Force Office of Scientific Research, and the Petroleum Research Fund, administered by the American Chemical Society, is gratefully acknowledged.

APPENDIX A: THE TEMPORAL PROFILE OF PHOTON ECHOES

The evaluation of the echo signal [Eq. (3)] involves a nontrivial triple integration [Eq. (4)]. In practice, we can partition all the system modes into fast and slow groups with respect to the time scales of the excitation pulses. This was recently applied to calculate the time-resolved pump probe absorption signal.[37] The fast modes are usually the high frequency optically active modes of the chromophore, while the slow modes consist of collective solvent motions as well as some low frequency chromophore modes. In the case of impulsive excitation, all the molecular modes are considered slow. To lowest order, we may factorize the molecular correlation function $R_j(t_3,t_2,t_1)$ into the fast and slow contributions. In the evaluation of the optical signal, it is more convenient to express the fast modes in terms of their vibronic levels since only a few of these levels are excited appreciatively. In the following, we shall denote $\hbar\omega_{vv'} \equiv \epsilon_v - \epsilon_{v'}$ as the energy difference between two vibronic levels of fast modes. With this notation, the echo polarization [Eq. (4)] may be expressed as

$$P^{(3)}_{\rm SPE}(\mathbf{k}_S,t) = i^3 \exp[i(\Omega_3+\Omega_2-\Omega_1-\omega_{eg})t + i(\Omega_2-\Omega_1)\tau - i(\Omega_1-\omega_{eg})\tau']$$
$$\times \sum_{a,b,c,d} P(a)\mu_{ab}\mu_{bc}\mu_{cd}\mu_{da}\exp(-i\omega_{dc}t + i\omega_{ba}\tau')$$
$$\times [\exp(-i\omega_{db}\tau - \gamma_{db}\tau) I(t-\tau';\omega_{bc},\omega_{da},\omega_{ba}) R'_2(t,\tau,\tau')$$
$$+ \exp(-i\omega_{ac}\tau - \gamma_{ac}\tau) I(t-\tau';\omega_{da},\omega_{bc},\omega_{ba}) R'_3(t,\tau,\tau')] \tag{A1}$$

with

$$I(t-\tau';\omega_{vv'},\omega_{\lambda\lambda'},\omega_{\kappa\kappa'}) \equiv \int_{-\infty}^{t} dt_3 \int_{-\infty}^{\tau+t_3} dt_2 \int_{-\infty}^{\tau'+t_2} dt_1\, \chi(t-\tau'-t_3-t_2+t_1) E_3(t_3) E_2(t_2) E_1^*(t_1)$$
$$\times \exp[i(\omega_{vv'}+\omega_{eg}-\Omega_3)t_3 + i(\omega_{\lambda\lambda'}+\omega_{eg}-\Omega_2)t_2 - i(\omega_{\kappa\kappa'}+\omega_{eg}-\Omega_1)t_1]. \tag{A2}$$

In deriving these equations, we changed the integration variables $t'_1 = t+\tau'+\tau-t_3-t_2-t_1, t'_2 = t+\tau-t_3-t_2$, and $t'_3 = t-t_3$. In Eq. (A1), R'_j denotes the contribution of the slow motion (excluding inhomogeneous broadening) to the molecular correlation function, $a,c,\ldots$, are the vibronic quantum numbers of the chromophore in ground electronic $|g\rangle$ state, whereas $b,d,\ldots$, are the vibronic quantum numbers in excited electronic $|e\rangle$ state. $P(a)$ is the thermal occupation of the chromophore in the vibronic level $|a\rangle$. γ_{db} (or γ_{ac}) represents the vibrational dephasing rate between $|d\rangle$ and $|b\rangle$ (or $|a\rangle$ and $|c\rangle$) levels. $\mu_{vv'} \equiv \langle v|\mu|v'\rangle$ is the Franck–Condon factor of the chromophore transition dipole moment. In Eq. (A1), we replaced the slow motion contribution $R'_j(t_3,t_2,t_1)$ by $R'_j(t,\tau,t)$, since the relevant time scales $|\tau'-t_1|$, $|\tau'-t_2|$ and $|t-t_3|$ are controlled by the excitation pulses. If the pulses are short compared to the inhomogeneous dephasing as well, we may further approximate $\chi(t_3-t_1)$ by $\chi(t-\tau')$. τ and τ' are the intervals between the excitation pulses, while t represents the time of the echo generated after the third pulse. We shall be interested in the experiment in which all the excitation pulses and the echo pulse are well separated. In this case, all three upper limits of the integrations in Eq. (A2), t, $\tau+t_3$ and $\tau'+t_2$, can be replaced by infinity, and we have

$$I(t-\tau';\omega_{vv'}\omega_{\lambda\lambda'},\omega_{\kappa\kappa'})$$
$$\equiv \int_{-\infty}^{\infty} d\omega \exp[-i\omega(t-\tau')]\hat{\chi}(\omega)$$
$$\times \hat{E}_3(\omega_{vv'}+\omega)\hat{E}_2(\omega_{\lambda\lambda'}+\omega)\hat{E}_1^*(\omega_{\kappa\kappa'}+\omega). \tag{A3}$$

Here, $\hat{\chi}(\omega)$ represents the inhomogeneous distribution:

$$\chi(t) = \int_{-\infty}^{\infty} d\omega \exp(-i\omega t)\hat{\chi}(\omega), \tag{A4}$$

and $\hat{E}_j(\omega)$ is the spectral envelope of the jth excitation field:

$$\hat{E}_j(\omega) = \int_{-\infty}^{\infty} dt \exp[i(\omega+\omega_{eg}-\Omega_j)t] E_j(t)$$
$$j = 1,2,3. \tag{A5}$$

In medium with large inhomogeneous broadening where the inhomogeneous dephasing time is short compared to all the other molecular dynamics, we can further replace $R'_j(t,\tau,\tau')$ in Eq. (A1) by $R'_j(\tau',\tau,\tau')$. Moreover, in the impulsive excitation limit, all the molecular modes are slow and can be incorporated in the correlation functions R'_2, R'_3, and I, so that the summations in Eq. (A1) can be eliminated. When both the large inhomogeneous broadening and the impulsive excitation limits are satisfied, the amplitude square of the polarization [Eq. (A1)], or the echo profile [the integrand of Eq. (3)], is given by

$$|P^{(3)}_{\rm SPE}(\mathbf{k}_S,t)|^2 = |\mathscr{R}(\tau',\tau,\tau')|^2 |I(t-\tau')|^2. \tag{A6}$$

Here, $I(t-\tau') \equiv I(t-\tau';\omega_{vv'}=\omega_{\lambda\lambda'}=\omega_{\kappa\kappa'}=0)$ represents the temporal profile of the echo. It can be shown that this profile centers at $t=\tau'$ with the width of $[(T_2^*)^2+\tau_1^2+\tau_2^2+\tau_3^2]^{1/2}$, where T_2^* and τ_j are the timescales of inhomogeneous dephasing and the jth excitation pulse, respectively. When the excitation pulses are short compared with the inhomogeneous dephasing, we may approximate $\hat{E}_j(\omega), j=1,2,3$, by constants. In this case $I(t-\tau')$ [Eq. (3.7)] reduces to $\chi(t-\tau')$, the inhomogeneous dephasing function. If only the impulsive limit is satisfied and the large inhomogeneous broadening does not hold, $R_j(\tau',\tau,\tau')$ in Eq. (A6) should be replaced by $R_j(t,\tau,\tau')$ which also contributes to the temporal profile of the echo pulse.[55]

Let us consider an ideal stimulated echo experiment for solvation dynamics, in which single-color echo pulses are used to excite the solvated chromophore at low temperature. In this case $\Omega_1 = \Omega_2 = \Omega_3$ and the initial Boltzmann distribution for the $P(0) = 1$ and $P(a) = 0$ for $a \neq 0$. We further assume there is a separation of time scales between the coherent motions of chromophore (fast modes) and the homogeneous dephasing or diffusion motions of solvent (slow modes). The excitation bandwidth $\hat{E}_j(\omega)$ is narrow compared to the vibronic level spacing $\omega_{vv'}$, the field function I [Eq. (A3)] selects only a single vibronic level (e.g., $|b\rangle$) in the excited state such that $b = d$ and $c = a$. In this case the amplitude square of the polarization [Eq. (A1)] reduces to

$$|P^{(3)}_{\mathrm{SPE}}(\mathbf{k}_S,t)| = |\mu_{ab}|^8 |\mathscr{R}'(t,\tau,\tau')|^2 \times |I(t-\tau';\omega_{ba},\omega_{ba},\omega_{ba})|^2. \quad \text{(A7)}$$

Here the molecular correlation functions $\mathscr{R}' \equiv R_2' + R_3'$ contains only the solvent contribution to $\mathscr{R}$, i.e., homogeneous dephasing and spectral diffusion processes but no contribution from intramolecular high frequency modes. If the inhomogeneous dephasing is fast compared with the solvent dynamics, we can further replace $\mathscr{R}'(t,\tau,\tau')$ in Eq. (A7) by $\mathscr{R}'(\tau',\tau,\tau')$.

APPENDIX B: THE INCOHERENT ACCUMULATED PHOTON ECHOES: DERIVATION OF EQ. (11)

We are interested in calculating the signal generated in the probe direction $\mathbf{k}_2$ and detected as a homodyne beat with the probe field. We have

$$\begin{aligned} S(\mathbf{k}_2;\tau') &= -2\,\mathrm{Im}\langle E^*(t)P^{(3)}(\mathbf{k}_S = \mathbf{k}_1 + \mathbf{k}_2 - \mathbf{k}_1, t)\rangle \\ &= 2\,\mathrm{Re}\int_0^\infty dt_3 \int_0^\infty dt_2 \int_0^\infty dt_1 \{\exp[i\Omega(t_3 - t_1)][F_2 + F_3]\mathscr{R}(t_3,t_2,t_1)\chi(t_3 - t_1)\} \\ &+ 2\,\mathrm{Re}\int_0^\infty dt_3 \int_0^\infty dt_2 \int_0^\infty dt_1 \{\exp[i\Omega(t_3 + t_1)][F_1 + F_4]\overline{\mathscr{R}}(t_3,t_2,t_1)\chi(t_3 + t_1)\}, \end{aligned} \quad \text{(B1)}$$

where

$$\begin{aligned} F_1 &= \langle E^*(t)E(t-t_3)E^*(t+\tau'-t_3-t_2)E(t+\tau'-t_3-t_2-t_1)\rangle \\ F_2 &= \langle E^*(t)E(t+\tau'-t_3)E(t-t_3-t_2)E^*(t+\tau'-t_3-t_2-t_1)\rangle \\ F_3 &= \langle E^*(t)E(t-t_3)E(t+\tau'-t_3-t_2)E^*(t+\tau'-t_3-t_2-t_1)\rangle \\ F_4 &= \langle E^*(t)E(t+\tau'-t_3)E^*(t+\tau'-t_3-t_2)E(t-t_3-t_2-t_1)\rangle. \end{aligned} \quad \text{(B2)}$$

In Eq. (B1), $\overline{\mathscr{R}}(t_3,t_2,t_1) \equiv R_1(t_3,t_2,t_1) + R_4(t_3,t_2,t_1)$ where R_1 and R_4 are molecular correlation functions, which can be obtained from R_2 [Eq. (5a)] and R_3 [Eqs. (5b)], respectively, by changing $\mathscr{G}_{ge}(t_1)$ to $\mathscr{G}_{eg}(t_1)$. In the derivation of Eq. (B1) we invoked the rotating wave approximation but we did not assume temporal separation of the pump and the probe, since it does not hold in the incoherent experiment [cf. Eq. (8)]. The four-time-correlation function F_α [Eqs. (B2)] can further be evaluated by assuming Gaussian statistics for the field and Eqs. (10). We then get

$$\begin{aligned} F_1 &= \theta(t_3 + t_2 + t_1 - \tau')\theta(\tau' - t_2) + \theta(t_3)\theta(t_1), \\ F_2 &= \theta^*(\tau' - t_3)\theta(\tau' - t_1) + \theta(t_3 + t_2)\theta^*(t_2 + t_1), \\ F_3 &= \theta(t_3 + t_2 - \tau')\theta^*(t_1 + t_2 - \tau') + \theta(t_3)\theta^*(t_1), \\ F_4 &= \theta^*(\tau' - t_3)\theta(\tau' + t_1) + \theta(t_3 + t_2 + t_1)\theta^*(t_2). \end{aligned} \quad \text{(B3)}$$

Not all of these terms contribute to the echo signal. Firstly, all the second terms of $F_j j = 1,\ldots,4$, contribute to the dc component of the signal, therefore, can be omitted. Further, the echo signal is generated only when τ_c, the time scale of the field correlation $\theta(t)$, is short compared with the dephasing time of the optical medium and the delay time τ' of the probe field from the pump field. In this case, both F_1 and F_4 have only negligible contributions to the ac component of the signal [Eq. (B1)]. We thus obtain the final expression for incoherent accumulated photon echo signal [Eq. (11)].

[1] R. G. Breene, *Theories of Spectral Line Shapes* (Wiley, New York, 1981).
[2] S. Mukamel, J. Chem. Phys. **71**, 2884 (1979); Phys. Rep. **93**, 1 (1982); S. Mukamel, Phys. Rev. A **28**, 3480 (1983).
[3] M. J. Weber, J. Lumin. **36**, 179 (1987).
[4] B. M. Kharlamov, R. I. Personov, and L. A. Bykovskaya, Opt. Commun. **12**, 191 (1974).
[5] Yu. T. Mazurenko and V. S. Udaltsov, Opt. Spectrosc. **44**, 417 (1977).
[6] E. W. Castner, M. Maroncelli, and G. R. Fleming, J. Chem. Phys. **86**, 1090 (1987); E. W. Castner, G. R. Fleming, B. Bagchi, and M. Maroncelli, *ibid.* **89**, 3519 (1988).
[7] J. Friedrich and D. Haarer, J. Chem. Phys. **76**, 61 (1982); J. Friedrich, J. D. Swalen, and D. Haarer, *ibid.* **73**, 705 (1980); G. Shulte, W. Grond, D. Haarer, and R. J. Silbey, **88**, 679 (1988).
[8] C. H. Brito-Curz, R. L. Fork, W. H. Knox, and C. V. Shank, Chem. Phys. Lett. **132**, 341 (1986).
[9] *Persistent Spectral Hole Burning: Science and Applications* edited by W. E. Moerner (Springer, Berlin, 1988).
[10] K. A. Nelson and E. P. Ippen, Adv. Chem. Phys. **75**, 1 (1989); Y. X. Yan, L. T. Cheng, and K. A. Nelson, *Advances in Nonlinear Spectroscopy*, edited by R. J. H. Clark and R. E. Hester (Wiley, New York, 1988), p. 299.
[11] J. Chesnoy and A. Mokhtari, Phys. Rev. A **38**, 3566 (1988); A. Mokhtari and J. Chesnoy, Europhys. Lett. **5**, 523 (1988).
[12] M. Mitsunaga and C. L. Tang, Phys. Rev. A **35**, 1720 (1987); I. A. Walmsley, M. Mitsunaga, and C. L. Tang, *ibid.* **38**, 4681 (1988).
[13] S. Saikan, Phys. Rev. A **38**, 4669 (1988); S. Saikan, T. Nakabayashi, Y.

Kenematsu, and A. Imaoka, J. Chem. Phys. **89**, 4609 (1980); S. Saikan, T. K. Shida, Y. Kanematsu, H. Aota, A. Harada, and M. Kanachi, Chem. Phys. Lett. **166**, 358 (1990).
[14] C. Kalpouzos, D. McMorrow, W. T. Lotshaw, and G. A. Kenney-Wallace, Chem. Phys. Lett. **155**, 240 (1989); *ibid.* **150**, 138 (1988); D. McMorrow, W. T. Lotshaw, and G. A. Kenney-Wallace, IEEE J. Quantum Electron **QE-24**, 443 (1988).
[15] H. L. Fragnito, J. Y. Bigot, P. C. Becker, and C. V. Shank, Chem. Phys. Lett. **160**, 101 (1989).
[16] N. A. Kurnit, I. D. Abella, and S. R. Hartmann, Phys. Rev. Lett. **13**, 567 (1964); I. D. Abella, N. A. Kurnit, and S. R. Hartmann, Phys. Rev. **141**, 391 (1966); T. W. Mossberg, R. Kachru, A. M. Flusberg, and S. R. Hartmann, Phys. Rev. A **20**, 1976 (1979).
[17] C. K. N. Patel and R. E. Slusher, Phys. Rev. Lett. **20**, 1087 (1968); J. P. Gordon, C. H. Wang, C. K. N. Patel, R. E. Slusher, and W. J. Tomlinson, Phys. Rev. **179**, 294 (1969).
[18] R. L. Shoemaker, Annu. Rev. Phys. Chem. **30**, 239 (1979); R. Brewer and R. L. Shoemaker, Phys. Rev. Lett. **27**, 631 (1971).
[19] T. Mossberg, A. Flusberg, R. Kachru, and S. R. Hartmann, Phys. Rev. Lett. **39**, 1523 (1977).
[20] H. W. H. Lee, F. G. Patterson, R. W. Olson, D. A. Wiersma, and M. D. Fayer, Chem. Phys. Lett. **90**, 172 (1982).
[21] J. B. W. Morsink, W. H. Hesselink, and D. Wiersma, Chem. Phys. **71**, 289 (1982).
[22] W. H. Hesselink and D. A. Wiersma, Phys. Rev. Lett. **43**, 1991 (1979); J. Chem. Phys. **73**, 648 (1980); in *Modern Problems in Condensed Matter Sciences*, edited by V. M. Agranovich and A. A. Maradudin (North-Holland, Amsterdam, 1983), Vol. 4, p. 249.
[23] S. Saikan, T. Nakabayashi, Y. Kanematsu, and A. Imaoka, J. Chem. Phys. **89**, 4609 (1988).
[24] E. L. Hahn, Phys. Rev. **80**, 580 (1950).
[25] A. Abragam, *The Principles of Nuclear Magnetism* (Clarendon, Oxford, 1961).
[26] L. Allen and J. H. Eberly, *Optical Resonance and Two-Level Atoms* (Wiley, New York, 1975).
[27] N. Bloembergen, E. M. Purcell, and R. V. Pound, Phys. Rev. **73**, 679 (1984); P. W. Anderson and P. R. Weiss, Rev. Mod. Phys. **25**, 269 (1953); R. Kubo, Adv. Chem. Phys. **15**, 101 (1969).
[28] R. F. Loring and S. Mukamel, Chem. Phys. Lett. **114**, 426 (1985).
[29] P. G. Wolynes, J. Chem. Phys. **86**, 5133 (1987).
[30] I. Rips, J. Klafter, and J. Jortner, J. Chem. Phys. **88**, 3246; **89**, 4288 (1988).
[31] R. F. Loring, Y. J. Yan, and S. Mukamel, J. Chem. Phys. **87**, 5840 (1987).
[32] A. L. Nichols and D. F. Calef, J. Chem. Phys. **89**, 3783 (1988).
[33] L. E. Fried and S. Mukamel, J. Chem. Phys. **93**, 932 (1990).
[34] W. R. Lambert, P. M. Felker, and A. M. Zewail, J. Chem. Phys. **75**, 5958 (1981).
[35] A. Mokhtari, J. Chesnoy, and A. Laubereau, Chem. Phys. Lett. **155**, 593 (1989).
[36] P. C. Becker, H. L. Fragnito, J. Y. Bigot, C. H. Brito-Cruz, R. L. Fork, and C. V. Shank, Phys. Rev. Lett. **63**, 505 (1989).
[37] Y. J. Yan and S. Mukamel, Phys. Rev. A **41**, 6485 (1990); W. B. Bosma, Y. J. Yan, and S. Mukamel, J. Chem. Phys. **93**, 3863 (1990).
[38] Y. J. Yan and S. Mukamel, J. Chem. Phys. (to be published).
[39] Y. R. Shen, *The Principles of Nonlinear Optics* (Wiley, New York, 1984).
[40] S. Mukamel and R. F. Loring, J. Opt. Soc. Am. B **3**, 595 (1986).
[41] Y. J. Yan and S. Mukamel, J. Chem. Phys. **89**, 5160 (1988).
[42] H. J. Eichler, P. Gunter, and D. W. Pohl, *Laser-induced Dynamic Gratings* (Springer, Berlin, 1986).
[43] Y. S. Bai and M. D. Fayer, Chem. Phys. **128**, 135 (1988); L. R. Narasimhan, K. A. Littau, D. W. Pack, Y. S. Bai, A. Elschner, and M. D. Fayer, Chem. Rev. **90**, 439 (1990).
[44] N. Morita and T. Yajima, Phys. Rev. A **30**, 2525 (1984).
[45] R. Beach and S. R. Hartmann, Phys. Rev. Lett. **53**, 663 (1984).
[46] S. Asaka, H. Nakatsuka, M. Fujiwara, and M. Matsuoka, Phys. Rev. A **29**, 2286 (1984).
[47] S. Mukamel, Annu. Rev. Phys. Chem. **41**, 647 (1990).
[48] Y. J. Yan, L. E. Fried, and S. Mukamel, J. Phys. Chem. **93**, 6991 (1989).
[49] S. Mukamel, Adv. Chem. Phys. **70**, 165 (1988); Y. J. Yan and S. Mukamel, J. Chem. Phys. **86**, 6085 (1987).
[50] S. Saikan, T. Nakabayashi, Y. Kanematsu, and N. Tato, Phys. Rev. B **38**, 7777 (1987).
[51] D. Froster, *Hydrodynamics Fluctuations, Broken Symmetry, and Correlation Functions* (Benjamin, New York, 1975), Chap. 2.
[52] S. A. Adelman and J. D. Doll, J. Chem. Phys. **63**, 4908 (1975); S. A. Adelman, *ibid.* **64**, 124 (1976).
[53] R. Benguria and M. Kac, Phys. Rev. Lett. **46**, 1 (1980).
[54] I. I. Markham, Rev. Mod. Phys. **31**, 956 (1959).
[55] W. Bosma, Y. J. Yan, and S. Mukamel, Phys. Rev. A (in press).